Neurocomputing 452 (2021) 768–778

Contents lists available at ScienceDirect

Neurocomputing

journal homepage: www.elsevier.com/locate/neucom

Towards online myoelectric control based on muscle synergies-to-force mapping for robotic applications ☆

Cristian Camardella [a,*], Michele Barsotti [a], Domenico Buongiorno [b,c,*], Antonio Frisoli [a], Vitoantonio Bevilacqua [b,c]

[a] PercRo Laboratory, Scuola Superiore Sant'Anna, Pisa, Italy
[b] Department of Electrical and Information Engineering, Polytechnic University of Bari, Bari, BA, Italy
[c] Apulian Bioengineering s.r.l., Via delle Violette n°14, Modugno, BA, Italy

ARTICLE INFO

Article history:
Received 16 April 2020
Revised 14 August 2020
Accepted 31 August 2020
Available online 19 December 2020

Keywords:
Myocontrol
Muscle synergies
Clustering
Upper limb
Exoskeleton
Prostheses

ABSTRACT

The development of a functional myoelectric control represents a big challenge within the researchers community, due to the complexity of mapping the user's movement intention onto the control signals. It is continuously gaining attention since it could be useful for building natural, intuitive and tailored human–machine interfaces. In this context, muscle synergies-based approaches are playing an important role since they may be useful to exploit the modular organization of the musculoskeletal system.

Muscle synergies-based myo-control schemes have shown promising results when they are trained and validated at the same limb pose. However, dealing with a muscle-to-force mapping variability across multiple limb poses remains an open challenge, thus keeping these techniques unusable in several real application scenarios, e.g. rehabilitation contexts.

In this paper, the authors propose a method able to compute the synergies-to-force mapping of a new limb pose by interpolation, with the knowledge of the synergies-to-force mapping related to a limited set of limb poses. The proposed interpolation-based approach has been evaluated on three different kind of mappings: muscle-to-force, "Pose-Shared" synergies-to-force and "Pose-Related" synergies-to-force. The muscle-to-force mapping considers a direct map between muscles and hand force. Both synergies-to-force approaches consider a map between muscle synergies and hand force, but, the "Pose-Shared" mapping assumes that the muscle patterns can be factorized using data coming from different limb poses, whereas the "Pose-Related" one assumes that each pose has its own set of muscle primitives that can be clustered together. The generalization capability of the proposed approach has been evaluated by comparing performances obtained in untrained conditions with the ones obtained in trained upper limb poses. Results showed that synergies-based approach substantially reduce the performance loss when tested on untrained upper-limb's poses, demonstrating that muscle synergies may be suitable to be shared across different working conditions. Moreover, the feasibility of the proposed approach has been preliminary tested in an online condition, demonstrating that the subject was able to accomplish the force task by controlling a virtual cursor with his muscular activations.

1. Introduction

In the era of the human-centered design, myoelectric control is continuously gaining attention since it allows for a natural, intuitive and tailored human–machine interface. Myoelectric control, or myo-control, consists in decoding the human motor intention, through the analysis of electromyographic signals (EMG), and computing a set of control signals that drive the machine the human is interacting with. The scientific research in EMG-based control has been mainly driven by the need for more intuitive prosthetic devices [23]. However, myo-electric schemes have also showed promising results when applied in different scenarios, featuring the simultaneous control of multiple degrees of freedom (DoF), e.g. the control of orthoses and exoskeletons [8,6,7].

Although the neuro-muscular theory behind the EMG signals generation hypothesizes the existence of applicable schemes

☆ This work has been partially founded by the PRIN-2015 ModuLimb (Prot. 2015HFWRYY) and supported by the Italian project RoboVir within the BRIC INAIL-2016 program.

* Corresponding authors at: Department of Electrical and Information Engineering, Polytechnic University of Bari, Bari, BA, Italy (D. Buongiorno).

E-mail addresses: cristian.camardella@santannapisa.it (C. Camardella), domenico.buongiorno@poliba.it (D. Buongiorno).

https://doi.org/10.1016/j.neucom.2020.08.081
0925-2312/

[14], still no robust and reliable solutions appeared among both scientific literature and commercial devices [1]. In the last decades, the biological inspired approaches have earned an increasing approval by the scientific community even though how the human central nervous system (CNS) copes with a complex neuromusculoskeletal system is not fully understood yet [12,28].

The bio-inspired myo-control paradigms could be mainly categorized in model-based and synergies-based approaches. The former relies on the mathematical modeling of all physiological and mechanical processes that are involved in the human movement generation and it is usually used to accurately estimate the articulations torque at the expense of both a long lasting calibration phase and high computational cost [7]. The latter aims at minimizing the computational cost by mimicking the CNS through the identification of specific muscle activation patterns, also called muscle synergies, exploited during task-related movements [3].

In the last decade, some researchers have focused their attention on the development of muscle synergies-based approaches for the human motor activity detection, that represents the basis for an effective myoelectric control [17]. For the sake of brevity, the two most representative papers are reported and described.

Denise Berger et al. [2] demonstrated that muscle synergies represented a valid technique to continuously estimate isometric forces generated by the hand in real-time through the surface EMG acquired from upper limb muscles. The setup proposed by Berger et al. considered a single arm pose and isometric forces applied at the hand in multiple directions on the horizontal plane. The authors demonstrated that the proposed synergies-based myo-controller was able to ensure the same level of accuracy achieved using the force sensor during online tasks. Ning Jiang et al. [19] successfully developed a strategy for achieving an accurate simultaneous and proportional control of a 2-Degrees of Freedom (DoF) wrist prostheses by concurrently extracting synergies-based control signals from each independent DoF. However, they documented a substantial decrease of the performance when introducing the 3rd DoF. In both the above mentioned works, the proposed setups for the experimental validation were based on a single arm/wrist pose and considered isometric multi-DOF forces generated at the hand/wrist. It is worth noting that the two cited works successfully proposed synergies-based myo-controllers that are able to estimate the human motor intention during tasks involving few DoFs and a fixed arm pose. However, to the best of the authors' knowledge, how such approaches might be extended for setups featuring a high number of limb poses has been not studied yet. In fact, the already proposed paradigms rely on a specific synergies-to-force mapping that has been computed in a pre-defined limb pose.

The research question faced in this paper is: do we need to compute a synergies-to-DOF mapping for each potential pose the limb might assume during the task? In particular, it is interesting understanding how to build new models that, after being trained in few fixed upper-limb poses, are able to estimate the force from EMG signals acquired in non-trained upper-limb poses (generalization capabilities). The authors hypothesize a potential usage of a linear interpolation on trained models, as a first and simple attempt to solve the previous mentioned problems. Moreover, since synergies represent a set of motor primitives, they might be suitable to be shared across different upper limb poses, eventually leading to interesting outcomes with respect to a full muscles-to-force mapping. In this work, the authors propose a method that, with the knowledge of the synergies-to-force mapping related to few limb poses, is able to compute the synergies-to-force mapping of a new upper limb pose through the interpolation of regression matrices. Upper-limb muscles activity and isometric hand forces have been acquired during virtual planar reaching tasks in different 3D points (or pose) of a large workspace ($60cm \times 30cm$). Then, for each tested point in the workspace, the synergies-to-force mapping computed with the data acquired in that specific pose has been compared with the synergies-to-force mapping computed with the novel proposed method. More in detail, the proposed interpolation-based approach has been evaluated with three different kind of mappings: muscle-to-force, pose-shared synergies-to-force and pose-related synergies-to-force. The muscle-to-force mapping considers a direct map between muscles and hand force. Both the synergies-to-force methods consider a map between muscle synergies and hand force with the only difference that the "Pose-Shared" assumes that the muscle patterns can be factorized using data coming from different points, whereas the "Pose-Related" assumes that each point has its own set of muscle primitives that can be clustered together with the synergies extracted in the other points [5]. This work extends a previous paper [9] under three main points: (I) the workspace in this study is three times bigger than the previous one; (II) a larger number of subjects is involved and (III) it also introduces a preliminary online evaluation session.

2. Materials and methods

2.1. Participants

Five right-handed healthy subjects (four males, aged 27.6 ± 2.6 years, weight 74.6 ± 7.6 kg) were involved in the study. At the moment of the experiment, they had not any previous experience with myo-electric controlled applications. All the experiments have been approved by the Ethical Review Board of Scuola Superiore Sant'Anna (Approval Number: 1292) and conducted following the World Medical Association (WMA) Declaration of Helsinki. All subjects signed the written consent form before joining the experiment.

2.2. Experimental setup

The experimental setup reported in Fig. 1 consisted of a) an anthropomorphic robot (UR5, Universal Robots [26]) featuring six DoFs, 50 N maximum payload and a cylindrical handle with a ATI Gamma six-axis force/torque sensor, featuring 65 N maximum payload on x/y axes and a 125 Hz sampling rate, b) an anti-gravity support for the upper-limb (a 2 DoF passive structure used for removing the tonic component from the EMG signals), c) an EMG acquisition system, featuring two gtec 8-channels biosignal amplifiers with customizable band-pass and notch built-in filters in a master–slave configuration and d) an head mounted display (the Oculus Rift HMD, Oculus [25]) to immerse the subject in a simple virtual reality (VR) environment, composed by a wooden house in the countryside and two fluctuating balls representing the controlled cursor and the task target.

In order to move the robot end-effector (EE) to the selected workspace positions, the reference robot joint angles have been set using the provided API. The distance between the subject and the robot was computed with respect to the base joint of the robot in such a way that the central point of the workspace was reachable with an elbow angle equal to 90 degrees (see Fig. 1). The muscular activations were acquired from 14 different muscles crossing the elbow and shoulder articulations: biceps short head (BI SH), biceps long head (BI LO), brachioradial (BRACH), triceps long head (TRI LONG), triceps lateral head (TRI LAT), deltoid anterior head (DELT A), deltoid medial head (DELT M), deltoid posterior head (DELT P), trapezius (TRAP), pectoralis major (PECT M), teres major (TER MAJ), infraspinatus (INFRASP), latissimus dorsi (LAT DORSI) and rhomboid (ROMB). After a careful skin preparation, disposable Ag/AgCl surface electrodes were placed by following the Surface

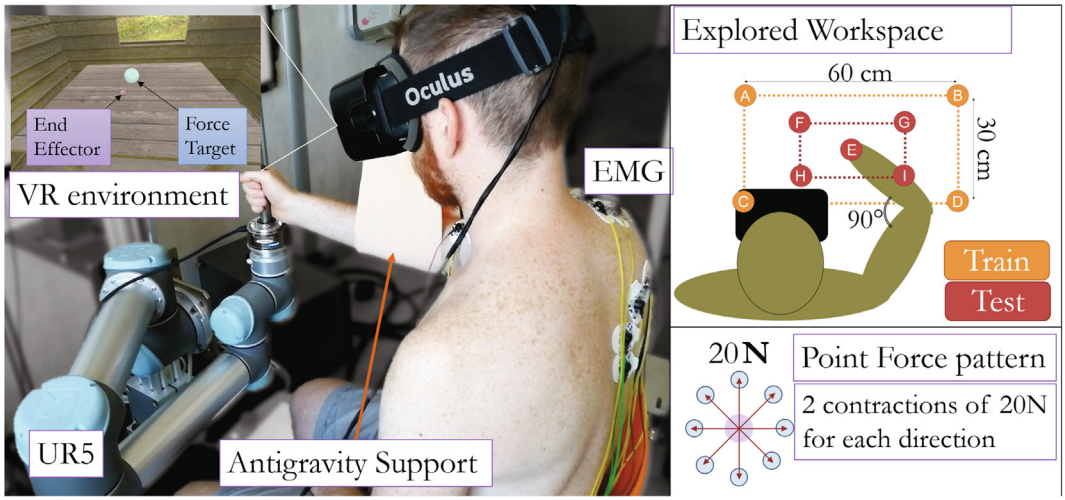

Fig. 1. Experimental setup. (Left) A Subject wearing VR glasses and the arm support. (Right-up) Positions of the nine evaluated 3D points/poses. (Right-bottom) Diagram of the forces patterns applied on each point.

EMG for Non-Invasive Assessment of Muscles (SENIAM) recommendations. Ground electrode was placed on the right elbow. The surface EMG signals were acquired using two bio-signals amplifiers (g.USBamp, gTec, Austria [15]) with a sampling frequency equal to 1200 Hz. All signals were filtered with a 5–600 Hz band-pass filter and a 50 Hz notch filter. The virtual engine and the force/torque sensor readings ran on a game-ready PC, whereas the EMG measurements and the acquisition routine ran in a host PC running Microsoft Windows 10 64 bit, Intel i7 1.73 GHz, 16 GB RAM and Matlab 2018b [24]. The synchronization of the force and EMG signals was achieved with a User Datagram Protocol (UDP) connection between the two PCs.

2.3. Data acquisition protocol

At the beginning of the experiment, after the EMG electrodes positioning, the subjects were invited to sit on a chair and the vertical position of the robot base was adjusted in order to place the EE handle by the sternum. The distance between the chair and the robot base was also adjusted such that the subjects were able to reach the central point E of the experimental workspace area with a elbow angle equal to 90 degrees (see Fig. 1). This distance, together with the low inter-subjects biometrical features variability (arm lenghts 33.6 ± 1.95, forearm lengths 28.6 ± 0.55) made the workspace suitable for all the subjects, avoiding arm singularities on the furthest points.

The evaluated area was delimited by a rectangle (60–30 cm^2) and included nine different 3D points (or arm poses) lying on the horizontal plane as shown in Fig. 1. For each of the nine points, subjects were asked to perform 16 reaching tasks along 8 directions (two trials per direction) equally spaced at 45 degrees and randomly sorted. Muscle contractions were performed isometrically by keeping the pose of the robot fixed with a position control. Once all 16 trials were completed, the robot automatically moved to another workspace point that was randomly selected. Each virtual reaching task consisted in 1) positioning the cursor, represented as a red sphere, inside the target, a blue sphere, 2) holding it in place for 2 s and then 3) relaxing, in order to move the cursor back to the rest position, for 2 more seconds. The position of the cursor was computed using a spring model $P_c = K * F_{EE}$, as shown in the work of Berger and D'Avella [2], where P_c is the 3D cursor position, F_{EE} is the applied isometric force vector and K is the elastic constant of the virtual spring. Considering this model, the rest position corresponded to a zero-force input. The target sphere had a bigger radius than the cursor radius such that a tolerance of 7 N was admitted.The force vector F_{EE} corresponded either to the measured force during the data acquisition phase or the force estimated by the EMG signals, during the online validation. Each trial started when the target sphere appears and ended when the target sphere disappeared.

2.4. Data analysis

The goal of this study is to build an EMG-to-Force model which, after being trained in few points placed at the vertexes of the predefined workspace, it is able to estimate the force inside the whole workspace. In the next paragraphs the words 'model' and 'regressor' (or 'regression matrix') are used as synonyms since the training phases are based on a linear regression on the collected datasets. Raw EMG signals were processed before feeding the training phase. They were rectified and filtered using a 4 Hz 2nd order Butterworth low-pass filter and then normalized using the maximum voluntary contraction (MVC) among all the channels within the whole dataset. Three different implemented *myocontrol approaches* have been called:

- Multi-variate linear regression (MVLR)
- Linear regression and "Pose-Shared" synergies (PSS)
- Linear regression and "Pose-Related" synergies (PRS)

A detailed description of the implemented approaches is provided in Section 3. The performance of each method have been compared in two different *conditions*:

- *Specific* condition: it consisted in estimating the hand-force on a workspace point using a regression model trained on the same point but using a different set of contractions. In particular, being each task composed by 2 contractions per direction (16 total), the dataset collected in a specific point was randomly split into 2 different datasets containing one contraction per direction each: one used for training the regressor and the other for testing the model.
- *General* condition: it was focused on understanding the quality of the estimations in a non-trained point by building the model out of the A-B-C-D training points and test it on the E-F-G-H-I points. For each of the three proposed methods, the model (i.e. the regression matrix) has been computed by linearly

interpolating the regression matrices trained in A-B-C-D. Consequently, the obtained regression matrix has been used to estimate the forces using EMG signals in the test points. The reason behind the use of A-B-C-D points only, in the training phase, lies on the possibility of building a linear space, i.e. a 5×5 points grid, on which those points could have been exploited as boundaries in the linear interpolation and, concurrently, choosing the smallest number of points, minimizing the required training data.

Data processing and conducted analysis always took into account the time window of a single virtual reaching trial, as described in the previous section, from the appearance of the target until the end of the rest phase. A summary of the analysis work-flow is showed in Fig. 2.

2.5. Online experiment

The aim of the online experiment was to assess and compare the performances of the proposed approaches in a real-time application in which the subject was involved in the control loop (receiving the feedback of the EMG-driven force estimation). Thus, pointing towards the actual usage of the myoelectric control, a pilot study has been conducted for evaluating the real-time estimation capabilities of the best offline algorithms. Starting from the same acquisition protocol (see Sub-Section 2.3), the online session has been performed by one subject, on a single point (i.e. point E): in this case, the cursor in the VR was driven by the online estimations, giving a direct visual feedback to the subject. Also the data processing replicated the same operations flow of the offline session. In this online study, the PRS method and the MVLR method have been evaluated both in Specific and General conditions.

2.6. Data analysis: performance indexes and statistics

Three different indexes have been used for assessing the performance of each method in each condition: Root Mean Square Error, Initial Angle Error and the Coefficient of Determination.

[A. Root Mean Square Error (*RMSE*)]
It is used to measure the difference between the measured and the estimated forces and it is calculated as follows:

$$RMSE = \frac{\sqrt{\frac{\sum_{i=1}^{N}\left(x_{x,i}^2 - \hat{x}_{x,i}^2\right)}{N}} + \sqrt{\frac{\sum_{i=1}^{N}\left(x_{y,i}^2 - \hat{x}_{y,i}^2\right)}{N}}}{2} \quad (1)$$

where x_i is the 2D measured force sample, made by its x and y component ($x_{x,i}$ and $x_{y,i}$), $\hat{x}_i$ is the 2D estimated output sample, made by its x and y component ($\hat{x}_{x,i}$ and $\hat{x}_{y,i}$) and N is the number of samples. Being the *RMSE* an error computation, the lower it is, the closer the estimation gets to the measured signal, in terms of signal amplitude.

[B. Initial Angle Error (*IAE*)]
The IAE index computes the difference between the measured and estimated 2D force angles using the last 70% of the rising edge of the signal after the contraction activation. It gives an indication about the correctness of the estimated force direction with respect to the measured one (IAE equal to zero means a perfect force components overlapping): although an high *RMSE* value could denote a bad estimation, a low IAE value denotes a correct force direction estimation, thus, varying the output gain could eventually lead to a good prediction.

[C. The coefficient of determination (R^2)]
The R^2 is used to highlight a signal total variation explained by the estimates. The R^2 is computed as follows:

$$R^2 = 1 - \frac{SS_{res}}{SS_{tot}} = 1 - \frac{\sum_{i=1}^{N}(x_i - \hat{x}_i)^2}{\sum_{i=1}^{N}(x_i - \bar{x}_i)^2}, \quad (2)$$

where x_i is the measured force sample and $\hat{x}_i^2$ is the estimated output sample. N is the number of samples. The index ranges from minus infinite to 1 (equal to 1 in case of perfect estimation with an error equal to zero).

In order to assess differences between the two experimental conditions (Specific and General), a 2-way ANOVA analysis, using as factors the Conditions (Specific, General) and Methods (MVLR, PRS, PSS), has been conducted for each performance index in each test point. In case of significant main effects, Bonferroni corrected post hoc analysis was conducted.

3. Theory

In this section, all the developed algorithms are described from a mathematical point of view, highlighting the main difference in including or not muscle synergies in the estimation process. Moreover the basis for comparisons are stated, detailing how the performance indexes are computed. Referring to the training and the test phases in the *Specific condition*, the related EMG datasets, used for the force estimations process, involve either the first or the second contraction (see acquisition protocol). Thus, different signals are

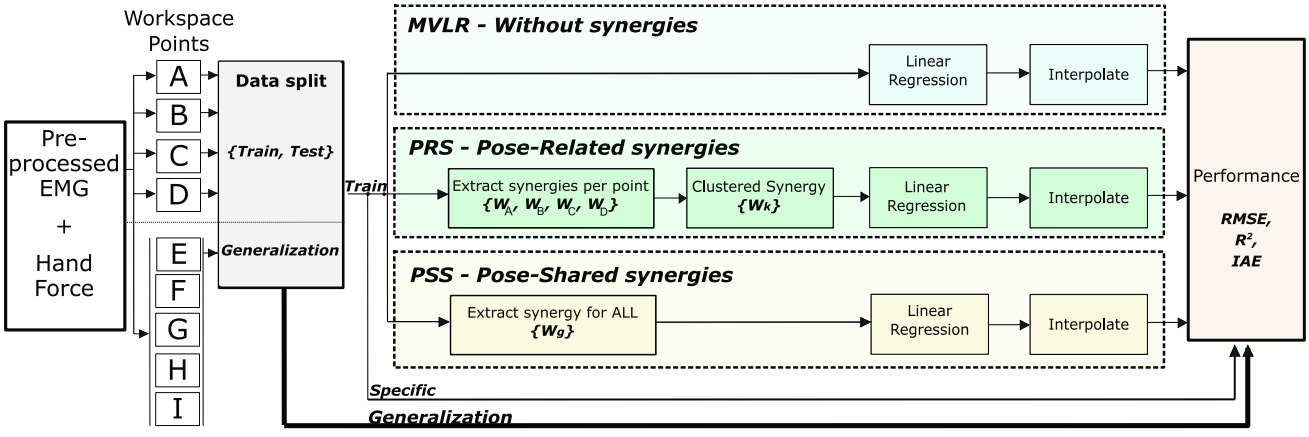

Fig. 2. Block diagram of the investigated control schemes.

always used even if the same point is used for both training and test phase.

3.1. Synergies extraction

Muscles synergies can be extracted from the electromyographical signals. Since a negative muscle activation has no physiological meaning, the Non-Negative Matrix Factorization (NNMF) [22] has been extensively used in order to separate the fundamental components from the input. According to the NNMF algorithm, muscle synergies can be expressed as following:

$$m = W \cdot c + e_m, \tag{3}$$

where m is the input signal (M-N matrix, being M the number of muscles and N the number of samples), W is the synergy matrix (M-s matrix, being s the number of synergies), c is the synergy activations matrix (s-N matrix) and e_m is the muscle activations factorization residuals, dimensionally equal to the input.

Depending on the input of the NNMF, two different approaches, namely *"Pose-Shared"* and *"Pose-Related"*, have been analyzed. The *"Pose-Shared"* synergies are extracted running the NNMF once on the EMG data acquired on all training arm poses (i.e. Points A, B, C and D) as follows:

$$m_T = W_g \cdot c_T + e_m, \tag{4}$$

where m_T is the union of the signals at the boundaries $m_T = [m_A \cup m_B \cup m_C \cup m_D]$ and W_g is the *"Pose-Shared"* synergy matrix.

The *"Pose-Related"* synergies are computed with a three steps procedure:

1. the NNMF factorization is independently applied on the EMG data recorded at each training arm pose producing four synergies matrices (W_i with i = 1:P, where P is the number of arm poses) with (3).
2. all the extracted synergies vectors are clustered using the K-means algorithm with cosine distance. For instance, given s the number of synergies and $W_i = [W_{i,1}, W_{i,2}, \ldots, W_{i,s}]$ the synergies matrix extracted on the i-th upper-limb pose and $W_{i,s}$ the s-th synergy (i.e. a vector) in the matrix, the k-means algorithm is used as follows:

$$W_{c,i} = kmeans([W_{1,i}, W_{2,i}, \ldots, W_{P,i}]), \quad i \in [1, s] \tag{5}$$

   where the output $W_{c,i}$ corresponds to the ith element of W_c matrix, as the ith centroid of the clustered synergies vectors.
3. The *"Pose-Related"* synergies matrix, W_c, can be computed as the union of all the s centroids:

$$W_c = [W_{c,1} \cup W_{c,2} \cup, \ldots, \cup W_{c,s}] \tag{6}$$

3.2. Force estimation

The performances of the proposed algorithms have been evaluated in terms of force estimation capabilities at both training and test upper-limb poses. The synergies-based methods have been compared with the state-of-art most common algorithm, i.e. linear regression using all the muscles activations. In this section an overview of the three approaches is presented. It is important to mention that muscles activations are always lower than the 20% of the value reached during the MVC and in each workspace position the arm's pose is fixed: following this, the relation between the force exerted at the hand and the EMG measured on the elbow and shoulder muscles is approximately linear [4,2,7]. For this reason, a linear regression has been used for each method.

[A. Multi-variate linear regression (MVLR)]

The algorithm that involves a direct relation between muscles activations and hand-force exertion has been used as a gold standard for the next comparisons, currently being the most used in the state of art. Under the linear condition previously mentioned, the force estimation can be computed using the following model:

$$F_{est}(t) = H_m \cdot m(t), \tag{7}$$

where $F_{est}(t)$ is the estimated 2-dimensional force, $m(t)$ is the processed EMG signal (made by all the channels) and H_m is the regression matrix calculated as:

$$H_m = reg(m_t, F_t) \tag{8}$$

where m_t is the training EMG data matrix (M-N where N is the number of samples) and F_t is the training forces data matrix (2-N matrix): thus, the H_m will be a 2-M matrix.

[B. Linear regression and *"Pose-Shared"* synergies (PSS)]

The concept of the *"Pose-Shared"* synergies is based on the difference in applying the factorization algorithm, i.e. NNMF, either on a pose-specific EMG dataset or on the data resulting from the union of more pose-specific datasets, as stated above. In the first case, the extracted synergies will suffer such an overfitting problem, testing them on points different from the training ones. In order to overcome the signal variability introduced by the joint angles differences in the new position, the second procedure has been used computing the *"Pose-Shared"* synergy matrix. The force estimation, thus, proceeds as follows:

$$F_{est}(t) = H_g \cdot c_g(t), \tag{9}$$

where $F_{est}(t)$ is the estimated 2-dimensional force, H_g is the regression matrix (2-s matrix, where s is the number of synergies) and $c_g(t)$ is the synergies activations matrix computed using 3 and neglecting the muscle residuals:

$$c_g = W_g^+ \cdot m, \tag{10}$$

where W_g^+ is the pseudo-inverse of W_g *"Pose-Shared"* synergy matrix seen in (4) and m is the filtered EMG signals matrix. Regarding the H_g regression matrix, it has been calculated as:

$$H_g = reg(c_{g,t}, F_t) \tag{11}$$

where $c_{g,t}$ is the c_g signal, computed using m_t, training EMG data matrix, as input of (10), and F_t is the training forces data matrix (matrices dimensions explained in paragraph A).

[C. Linear regression and "Pose-Related" synergies (PRS)]

The authors observed that in an extended region of the upper-limb workspace, point-specific muscle synergies capture in a better way the variation of the relative muscle weights, with respect to the points-shared ones [9]. A cluster analysis (*k-means* of all the point-specific synergies matrices, as done in paragraph 2.4) has been performed in order to obtain a resultant matrix which is supposed to have a better generalization capability with respect to the single ones. Eventually the estimation can be computed using the following formula:

$$F_{est}(t) = H_c \cdot c_c(t), \tag{12}$$

where $F_{est}(t)$ is the computed 2-dimensional force, H_c is the regression matrix (2-s matrix, where s is the number of synergies) and $c_c(t)$ is the synergies activations matrix computed using the inverse formula of (3) and neglecting the muscle residuals:

$$c_c = W_c^+ \cdot m, \tag{13}$$

where W_c^+ is the pseudo-inverse of W_c clustered synergies matrix as stated in (5) and m is the filtered EMG signals matrix. Also in this

Table 1
Algorithms and experiments summary. In 'Lin.Reg.' and 'Test' columns, 1st and 2nd stand for first contraction and second contraction of point-specific dataset. The table does not show the training performance extraction process (first column of Fig. 3).

Method	*Condition*	*Lin.Reg.matrix*(H)	*Syn.matrix*(W)	*Test*
MVLR	Specific	Calc. in EFGHI points (1st)	Not used	Est. in EFGHI (2nd)
MVLR	General	Calc. in ABCD points and interp.	Not used	Est. in EFGHI
PSS	Specific	Calc. in EFGHI points (1st)	Calc. in [A∪B∪C∪D]	Est. in EFGHI (2nd)
PSS	General	Calc. in ABCD points and interp.	Calc. in [A∪B∪C∪D]	Est. in EFGHI
PRS	Specific	Calc. in EFGHI points (1st)	Calc. in ABCD and clustered	Est. in EFGHI (2nd)
PRS	General	Calc. in ABCD points and interp.	Calc. in ABCD and clustered	Est. in EFGHI

case, the H_c regression matrix computation follows the same procedure:

$$H_c = reg(c_{c,t}, F_t) \tag{14}$$

where $c_{c,t}$ is the c_c signal, computed using m_t, training EMG data matrix, as input of (13), and F_t is the training forces data matrix.

3.3. Algorithms summary

In the previous paragraphs, all the proposed methods have been detailed from a mathematical and conceptual point of view. For the sake of clearness, the computation process is listed below with a step-by-step procedure, starting from the raw EMG signals processing, up to the force estimation, for each method.

Algorithm 1: Algorithms operations list. Once processed all the signals and extracted all the synergies matrices (W_i), *"Pose-Shared"* synergies (W_g) are extracted using all the training EMG signals and *"Pose-Related"* synergies (W_c) clustering all the W_i, as explained previously. Finally all the models (H) are trained and used in the estimation phase. It is important specifying that there are no distinctions between *Specific* and *General* conditions herein (see Table 1).

```
% Processing for both train/test data;
m_r = rawEMG;
m_f = filtering(m_r);
m_a = abs(m_f);
m = envelope(m_a);
% Training phase (m = m_train);
W_i = NMF(m_i), i ∈ [A, B, C, D], for each point;
W_c = kmeans([W_A, W_B, W_C, W_D]), once;
W_g = NMF([m_A, m_B, m_C, m_D]), once;
if algorithm=='PRS' then
    c_c=W_c^+*m;
    H_c = linreg(F,c_c);
else if algorithm=='PSS' then
    c_g=W_g^+*m;
    H_g = linreg(F,c_g);
else
    H_m = linreg(F,m);
end
% Estimation phase (m = m_test);
if algorithm=='PRS' then
    c_c=W_c^+*m;
    F_est = H_c*c_c;
else if algorithm=='PSS' then
    c_g=W_g^+*m;
    F_est = H_g*c_g;
else
    F_est = H_m*m;
end
```

A summary of the proposed algorithms logic and how the have been used in this study is reported in Algorithm 1.

4. Results

As reported in author's previous works [9,5], and in line with the works of D'Avella et al. [2,13], the authors found that a small number of synergies, with respect to the number of acquired muscles, was sufficient for building a functional subset of grouped muscles. In this work, five synergies have been selected for reconstructing the muscle activations, as found to be enough for representing more than the 90% of the variance of the EMG signals in a similar task [9,5]. Regarding the generalization capabilities of the proposed approaches, our initial hypothesis was that synergies-based techniques could have flattened the difference with MVLR, passing from *Specific* to *General* condition, since the extracted primitives could have been shared across different upper limb poses in a better way, with respect to a point specific muscles-to-force mapping. Fig. 3 reports the comparison between the performance obtained by the three explored methods (MVLR, PSS, PRS) under the two analyzed conditions (Specific (S) and General (G)). Each row is related to a different performance index. For the sake of completeness, the first column ("Training Points") shows the test performance in the training points (A B C D) under the *Specific condition*, i.e. the models have been trained on one half of the contractions and tested in the remaining ones. Each of the remaining columns ("Point X") reports the performance obtained in the test points (E F G H I) in both the *Specific condition* and the *General condition*, in which the models have been trained using datasets coming from the training points (A B C D) and tested in the specific column-point. An important note is that, differently from the regression matrix, that varied across conditions, the synergies used for the PSS and PRS methods were extracted once from the training points (see algorithms operation list) and never changed across the test points (E F G H I). In the upper part of each graph, statistical significances are reported. The gray long lines with asterisks show the significance of the 2-way ANOVA for the Condition factor (the significance of the Methods factor is not reported). In order to report graphically the differences between methods, black lines show the multiple comparisons between once the "Conditions" factor was fixed. In all the test points and for all the evaluated performance indexes (except for the IAE in points F and I), a significant difference has been found between the *Specific* and *General* conditions (RMSE: $F(1,24) > 17, p < 0.001$; $R^2 : F(1,24) > 10, p < 0.01$).

As can be observed, the error for the MVLR increases by almost 2 N when passing from the *Specific condition* to the *General* one, whereas the error increment for the synergy-based methods (PSS, PRS) is about 1 N. In particular, for both error-related performance (RMSE and IAE), the ratios of the errors in the *General condition* on the *Specific condition* are approximately 1.8 for the MVLR and 1.3 for both the PRS and PSS methods.

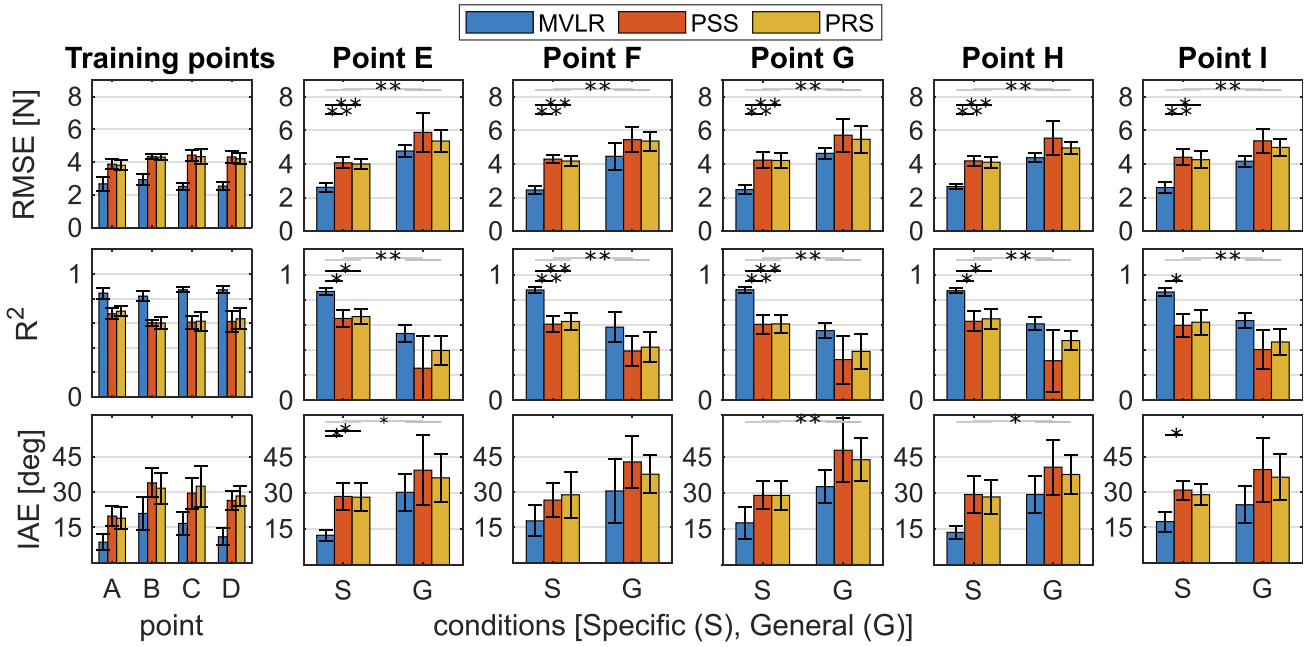

Fig. 3. Offline analysis performance. The three rows represent the computed performance (RMSE, R^2, IAE). The three colors represent the experimental methods. First columns graphs report the performance obtained in the training points (*Specific condition* only). The remaining columns report the performance in the test points both in the *Specific condition* (model trained in the same point) and in the *General condition* (model trained in A,B,C,D points and interpolated). Gray horizontal lines with asterisks over the bars report a significant difference between the *Specific* and *General* conditions. Black horizontal lines with asterisks report significant difference between methods inside each condition.

Interestingly, observing the statistical comparison between methods inside each condition (black lines in Fig. 3), it can be noted that significant differences between the MVLR and the synergy-based methods occur in almost all the cases in the *Specific condition* (RMSE: $F(1,12) > 10, p < 0.01$), whereas they never occur in the *General condition* (RMSE: $F(1,12) < 3, p > 0.05$). In fact, as outlined before, the decrement in performance between the *Specific condition* and *General condition* is higher when using all the muscles as input for the linear regressor (MVLR method) than when grouping muscles in synergies (PSS and PRS methods).

When comparing the synergies-based methods, although not really significant, it can be noted from Fig. 3 that the PRS method, which was computed by clustering the synergies extracted in each of the training point, always outperforms the PSS method, which was based on extracting synergies from the whole set of training points. The difference between the two synergistic methods is even more appreciable in the *General condition*. The difference between the two methods in terms of interpolated regression matrices can be observed in Fig. 4. It can be noted that, even if the two set of synergies are very similar, the generated force-fields show different behaviours on the workspace.

4.1. Online preliminary results

As mentioned above, an online session has been performed by one subject in the central point E, using both PRS and MVLR methods, and in the *Specific* and *General* conditions. A representative real-time force reconstruction is shown in Fig. 5. More in detail, the left panel of the figure shows the actual trajectories (the reaching phase only) of the measured force (force sensor, blue) and the online estimations (EMG-driven, red), and the force targets, depicted as green balls with the predefined force tolerance. It has to be considered that the subject could only see the EMG-estimated force during the online experiment. The right panel shows the whole ongoing EMG-estimated force and the measured force, split for the horizontal and vertical component, for eight consecutive contractions (reaching and back phases are included).

Table 2 reports the overall online performance, computed over the whole trajectories, based on the same indexes used for the offline analysis. The preliminary results showed that, even if there is a slight performance loss switching to the online usage, the subject was able to accomplish the task and control the EMG-driven force cursor. Obviously, in order to get more significant results, a higher number of subject is needed. Both methods allowed the user to reach 6 out of 8 total targets, without reporting a substantial difference switching from one method to the other. However, it can be observed that, whereas the error increasing on the synergies-based method remains the same as the offline analysis, when passing from the *Specific condition* to the *General condition*, this is not true for the MVLR method in which the error is almost the same in the two conditions.

5. Discussion and conclusions

This work presents an extended study (with respect to a previous work [9]) on the generalization abilities of different myoelectric control methods in a large upper-limb workspace (60 cm × 30 cm). The aim of the study was building a myoelectric control scheme that, after being trained on a reduced set of points placed at the vertexes of a rectangle drawn on the horizontal plane, was able to estimate the force at the hand in untrained points placed inside the rectangle. The offline results obtained in the study demonstrated the potentiality of synergies-based methods to be more robust against working conditions other than the training ones. Furthermore, this study also reports preliminary results of a real-time virtual control, in which the subject received the feedback of the EMG-driven estimations through the virtual environment, confirming the feasibility of the proposed approach.

As expected, the performance obtained in the same points the models were trained on (*Specific condition*) were significantly higher than performance obtained outside of the trained points

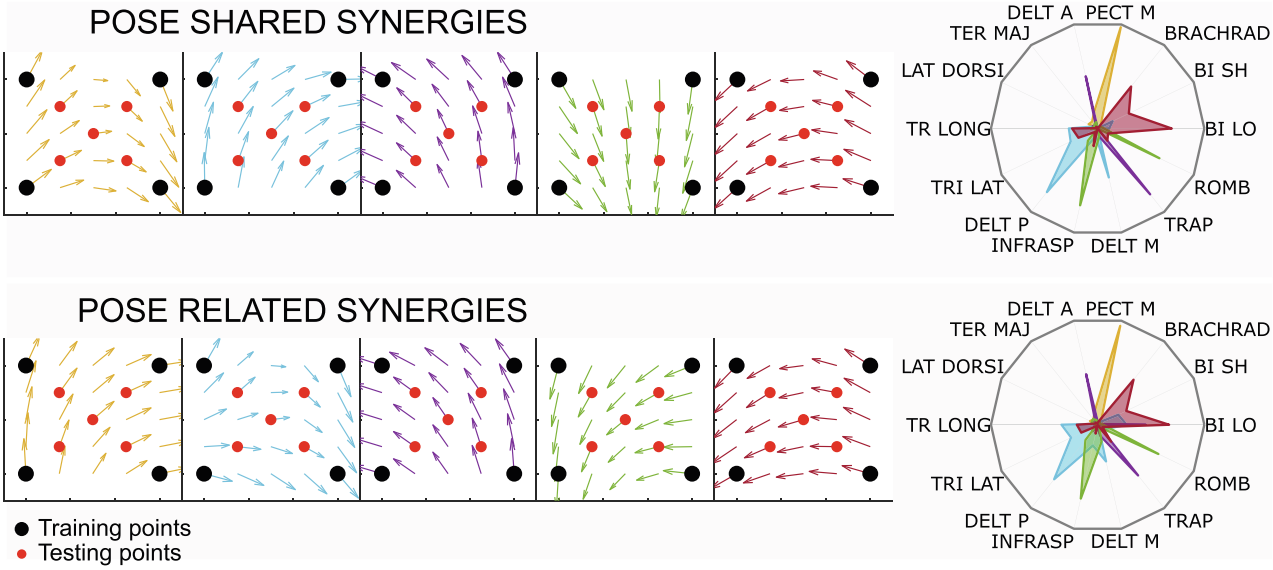

Fig. 4. Force fields and synergies for the two proposed methods. The force fields represent the interpolated regression matrices for each synergy. The color of the synergies match the color of the arrows in the force field.

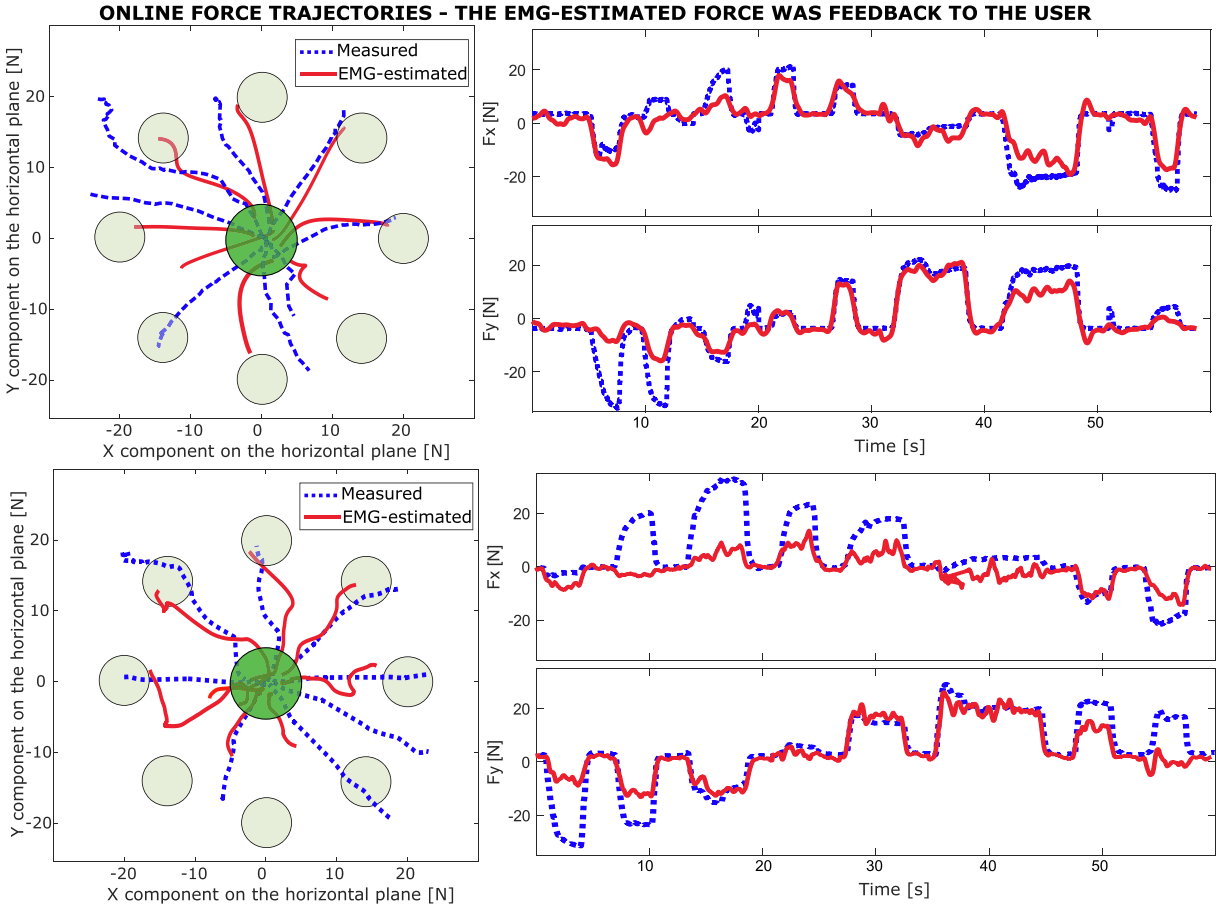

Fig. 5. Online representative force trajectory. The 2-D and the ongoing force profiles are depicted for the MVLR method (*General* condition) on the upper figure and for the PRS method (*General* condition) on the lower figure. The subject could see only effect of the EMG-estimated force (online feedback).

(*General condition*). Interestingly, concerning the comparison between the proposed force-estimation methods, significant differences were found in the *Specific condition* whereas no differences emerged in the *General condition*. More in detail, the MVLR method, which took as input the whole muscle space, always outperformed the synergy-based methods when tested in the *Specific condition* (same training point) but no significant differences between methods have been found when testing in out-of-training points (*Gen-*

Table 2
Online performance obtained by one subject in the four experimental conditions.

Method	*Condition*	*RMSE*[*N*]	R^2	*IAE*[*deg*]
MVLR	Specific	3.58	0.77	22.05
MVLR	General	3.30	0.79	16.54
PRS	Specific	5.70	0.61	18.36
PRS	General	7.34	0.57	29.66

eral condition). The authors thus hypothesize that the possibility to build a functional low-dimensional myoelectric controller, exploiting muscle synergies, strongly depends on the availability or not of a wide training set. In fact, as reflected in Fig. 3, having many training points spread across the upper-limb workspace, inevitably leads to better performances when using a point-specific algorithm without the reduction of the muscle space than when grouping muscles through synergies. Then, the results of this study have demonstrated that, when the training points are limited, the use of synergies-based approach leads to similar myo-control performance than using the whole set of muscles.

Among the proposed synergy-based algorithms, the *"Pose Related"* approach outperforms the *"Pose Shared"* one in all the points and conditions. Looking at the synergies force fields (see Fig. 4), although the PSS and PRS patterns share the same structure, for the PSS, the interpolation output appears more regular. This could be due to the fact that the *"Pose Shared"* synergies extraction took into account the overall variations of muscles activations in the whole training set. The *"Pose Related"* synergies may instead capture those point-specific features of electromyographical signals that eventually have led to a better force reconstruction.

The obtained results also demonstrated that a limited training set could be sufficient in order to obtain a model with good generalization capabilities outside the trained upper-limb configuration. This fact is of particular importance for real myocontrol application, since decreasing the time required to train the system is desirable in all human-interface systems and especially crucial in rehabilitation scenarios, where a shorter training phase results in more time for the effective therapy. Moreover, the application of muscle synergies has gained particular attention in the robot-assisted rehabilitative setting [11], in which they can provide the basis for developing and promoting targeted therapies for reinforcing neural plasticity: the customization of therapies, such that the abnormal muscles synergies can be detected and treated in favor of restoring the physiological structure and recruitment, is still an ongoing open challenge [10,27,18]. However, even though the use of synergies appears to be a promising solution, further investigations are needed especially in terms of real time applications.

The aim of the preliminary online experiment was to test the feasibility of the proposed approach in a real-time application and make a direct comparison between offline and online performances. Looking at the example trajectories (see Fig. 5), it can be noted that using MVLR in the *General condition* has led to a myoelectric control with performance comparable to the state-of-art. The methods used in this phase were the MVLR and PRS, the ones with the best performance according to the offline outcome. Observing Table 2, it can be noted that, while the RMSE differs between offline and online performances in the point E, the IAE does not. This means that the direction of the force is detected in the same way but the amplitude needs a custom adjustment. However, a deeper online testing is needed since only one subject has tried it. Moreover, being the online phase a feasibility test, no accurate analysis on the best online input signal filtering has been conducted. One well-known problem in myo-control applications concerns the delay between the user input and the control signal, that requires a dedicated study on the best trade-off between the amount of noise in the output and the delay that results from the filtering. In this preliminary study, the signal processing followed standard operations in the state-of-art, within similar contexts (i.e. myo-control).

Regarding the EMG-to-force mapping, the linear regressor has been selected as the last stage of the force estimation process. In fact, in the last years, efforts have been also put in investigating whether more complex regressor models (such as non-linear kernel ridge regressor, KRR), could overcome the most commonly used linear approach. Hahne et al. [16] systematically compared linear and non-linear regression techniques for a simultaneous and proportional myoelectric control of 2-DOF wrist movements. In their offline evaluation they have found that the non-linear methods outperformed the linear one. Similarly, Krasoulis et al. [21], in the context of fingers myo-control, showed in an offline analysis a superior performance in predicting trained finger movements with the non-linear KRR over the linear ridge regression. However, they also reported that, when generalizing to novel movements, the performance of the two regressors types were comparable. It is important to note that all these studies were performed offline, and, as it has been demonstrated by Jiang et al. [20], these findings do not necessarily mean that real-time performance will be effectively different. In fact, the quality of an online myoelectric control depends more on the continuous interaction and adaptation of the user with the myoelectric controller rather than on the high accuracy in the offline mapping between actual and estimated force. In conclusion this work sets the stage for a potentially functional synergies-based myo-control and opens the doors to future analysis on more complete real-time performance tests, trying to include also a true man-in-the-loop experiment with a robotic-assistive device.

CRediT authorship contribution statement

Cristian Camardella: Conceptualization, Methodology, Software, Validation, Visualization, Formal analysis, Investigation, Data curation, Writing - original draft, Writing - review & editing. **Michele Barsotti:** Conceptualization, Methodology, Validation, Visualization, Formal analysis, Investigation, Writing - original draft, Writing - review & editing. **Domenico Buongiorno:** Conceptualization, Methodology, Validation, Formal analysis, Investigation, Writing - original draft, Writing - review & editing. **Antonio Frisoli:** Conceptualization, Supervision, Project administration, Funding acquisition, Writing - review & editing. **Vitoantonio Bevilacqua:** Conceptualization, Supervision, Project administration, Funding acquisition, Writing - review & editing.

Declaration of Competing Interest

The authors declare that they have no known competing financial interests or personal relationships that could have appeared to influence the work reported in this paper.

References

[1] P. Beckerle, G. Salvietti, R. Unal, D. Prattichizzo, S. Rossi, C. Castellini, S. Hirche, S. Endo, H.B. Amor, M. Ciocarlie, et al., A human–robot interaction perspective on assistive and rehabilitation robotics, Front. Neurorobot. 11 (2017) 24, https://doi.org/10.3389/fnbot.2017.00024.
[2] D.J. Berger, A. d'Avella, Effective force control by muscle synergies, Front. Comput. Neurosci. 8 (2014) 46, https://doi.org/10.3389/fncom.2014.00046.
[3] E. Bizzi, A. d'Avella, P. Saltiel, M. Tresch, Book review: modular organization of spinal motor systems, Neuroscientist 8 (2002) 437–442, https://doi.org/10.1177/107385802236969.
[4] T.S. Buchanan, D.G. Lloyd, K. Manal, T.F. Besier, Neuromusculoskeletal modeling: estimation of muscle forces and joint moments and movements from measurements of neural command, J. Appl. Biomech. 20 (2004) 367–395, https://doi.org/10.1123/jab.20.4.367.

[5] D. Buongiorno, F. Barone, D.J. Berger, B. Cesqui, V. Bevilacqua, A. d'Avella, A. Frisoli, Evaluation of a pose-shared synergy-based isometric model for hand force estimation: towards myocontrol, in: Converging Clinical and Engineering Research on Neurorehabilitation II, Springer, 2017, pp. 953–958, https://doi.org/10.1007/978-3-319-46669-9_154.
[6] D. Buongiorno, F. Barone, M. Solazzi, V. Bevilacqua, A. Frisoli, A linear optimization procedure for an emg-driven neuromusculoskeletal model parameters adjusting: validation through a myoelectric exoskeleton control, in: F. Bello, H. Kajimoto, Y. Visell (Eds.), Haptics: Perception, Devices, Control, and Applications, Springer International Publishing, Cham, 2016, pp. 218–227, https://doi.org/10.1007/978-3-319-42324-1_22.
[7] D. Buongiorno, M. Barsotti, F. Barone, V. Bevilacqua, A. Frisoli, A linear approach to optimize an emg-driven neuromusculoskeletal model for movement intention detection in myo-control: a case study on shoulder and elbow joints, Front. Neurorobot. 12 (2018) 74, https://doi.org/10.3389/fnbot.2018.00074.
[8] D. Buongiorno, M. Barsotti, E. Sotgiu, C. Loconsole, M. Solazzi, V. Bevilacqua, A. Frisoli, A neuromusculoskeletal model of the human upper limb for a myoelectric exoskeleton control using a reduced number of muscles, in: 2015 IEEE World Haptics Conference (WHC), 2015, pp. 273–279, https://doi.org/10.1109/WHC.2015.7177725.
[9] C. Camardella, M. Barsotti, L.P. Murciego, D. Buongiorno, V. Bevilacqua, A. Frisoli, Evaluating generalization capability of bio-inspired models for a myoelectric control: a pilot study, in: International Conference on Intelligent Computing, Springer, 2019, pp. 739–750. 10.1007/978-3-030-26766-7_67..
[10] V.C. Cheung, A. Turolla, M. Agostini, S. Silvoni, C. Bennis, P. Kasi, S. Paganoni, P. Bonato, E. Bizzi, Muscle synergy patterns as physiological markers of motor cortical damage, Proc. Nat. Acad. Sci. 109 (2012) 14652–14656, https://doi.org/10.1073/pnas.1212056109.
[11] M. Coscia, P. Tropea, V. Monaco, S. Micera, Muscle synergies approach and perspective on application to robot-assisted rehabilitation, in: Rehabilitation Robotics, Elsevier, 2018, pp. 319–331. 10.1016/B978-0-12-811995-2.00024-2.
[12] A. d'Avella, M. Giese, Y.P. Ivanenko, T. Schack, T. Flash, Modularity in motor control: from muscle synergies to cognitive action representation, Front. Media SA (2016), https://doi.org/10.3389/fncom.2015.00126.
[13] A. d'Avella, A. Portone, L. Fernandez, F. Lacquaniti, Control of fast-reaching movements by muscle synergy combinations, J. Neurosci. 26 (2006) 7791–7810, https://doi.org/10.1523/JNEUROSCI.0830-06.2006.
[14] D. Farina, I. Vujaklija, M. Sartori, T. Kapelner, F. Negro, N. Jiang, K. Bergmeister, A. Andalib, J. Principe, O.C. Aszmann, Man/machine interface based on the discharge timings of spinal motor neurons after targeted muscle reinnervation, Nat. Biomed. Eng. 1 (2017) 0025, https://doi.org/10.1038/s41551-016-0025.
[15] gtec, g.tec medical engineering gmbh. https://www.gtec.at/product/g-usbamp-research/..
[16] J.M. Hahne, F. Biessmann, N. Jiang, H. Rehbaum, D. Farina, F.C. Meinecke, K.R. Müller, L.C. Parra, Linear and nonlinear regression techniques for simultaneous and proportional myoelectric control, IEEE Trans. Neural Syst. Rehabil. Eng. 22 (2014) 269–279, https://doi.org/10.1109/TNSRE.2014.2305520.
[17] M. Ison, P. Artemiadis, The role of muscle synergies in myoelectric control: trends and challenges for simultaneous multifunction control, J. Neural Eng. 11 (2014), https://doi.org/10.1088/1741-2560/11/5/051001 051001.
[18] S. Israely, G. Leisman, C.C. Machluf, E. Carmeli, Muscle synergies control during hand-reaching tasks in multiple directions post-stroke, Front. Comput. Neurosci. 12 (2018) 10, https://doi.org/10.3389/fncom.2018.00010.
[19] N. Jiang, K.B. Englehart, P.A. Parker, Extracting simultaneous and proportional neural control information for multiple-dof prostheses from the surface electromyographic signal, IEEE Trans. Biomed. Eng. 56 (2009) 1070–1080, https://doi.org/10.1109/TBME.2008.2007967.
[20] N. Jiang, I. Vujaklija, H. Rehbaum, B. Graimann, D. Farina, Is accurate mapping of emg signals on kinematics needed for precise online myoelectric control?, IEEE Trans. Neural Syst. Rehabil. Eng. 22 (2013) 549–558, https://doi.org/10.1109/TNSRE.2013.2287383.
[21] A. Krasoulis, S. Vijayakumar, K. Nazarpour, Evaluation of regression methods for the continuous decoding of finger movement from surface emg and accelerometry, in: 2015 7th International IEEE/EMBS Conference on Neural Engineering (NER), 2015, IEEE, pp. 631–634. 10.1109/NER.2015.7146702.
[22] D.D. Lee, H.S. Seung, Learning the parts of objects by non-negative matrix factorization, Nature 401 (1999) 788, https://doi.org/10.1038/44565.
[23] M. Markovic, M.A. Schweisfurth, L.F. Engels, D. Farina, S. Dosen, Myocontrol is closed-loop control: incidental feedback is sufficient for scaling the prosthesis force in routine grasping, J. Neuroeng. Rehabil. 15 (2018) 81, https://doi.org/10.1186/s12984-018-0422-7.
[24] Mathworks, The mathworks, inc. https://it.mathworks.com/products/matlab.html..
[25] Oculus, Facebook technologies llc. https://www.oculus.com/rift/..
[26] U. Robots, Universal robots a/s. https://www.universal-robots.com..
[27] J. Roh, W.Z. Rymer, R.F. Beer, Evidence for altered upper extremity muscle synergies in chronic stroke survivors with mild and moderate impairment, Front. Human Neurosci. 9 (2015) 6, https://doi.org/10.3389/fnhum.2015.00006.
[28] S. Tang, M. Barsotti, F. Stroppa, A. Frisoli, X. Wu, W. Hou, Upper limb joint angular velocity synergies of human reaching movements, in: 2018 IEEE International Conference on Cyborg and Bionic Systems (CBS), 2018, IEEE, pp. 641–646. 10.1109/CBS.2018.8612235.

Cristian Camardella is a PhD Student from Scuola Superiore Sant'Anna in Perceptual Robotics. He received the bachelor and master degree in Automation Engineering from Polytechnic University of Bari in 2017. In 2019 he was a visiting student at the Chinese University of Hong Kong, in collaboration with Prof. Raymond Tong on the post-stroke muscle synergies analysis and rehabilitation robotics strategies development. His interests cover the development of human-machine interfaces, bio-signals processing, robotics, machine learning and control strategies. Within these topics, he worked on muscle synergies and myoelectric control applications, in the rehabilitation context, as one of the main research topic.

Michele Barsotti received the bachelor and master degree (M.Sc.) in Biomedical Engineering from the University of Pisa in 2009 and 2011 respectively. He obtained his PhD degree in Emerging Digital Technologies from the Scuola Superiore Sant'Anna of Pisa on October 27th, 2016 with a dissertation on "Human-Machine interfaces based on electro-biological signals for robotic application and neurorehabilitation" with the final evaluation score of full marks and honor. In 2016 he was a visiting student at the Institute of Neurorehabilitation Systems at the University Medical Center G?ttingen, Georg-August University, Germany. He works as a post-doc researcher at the PercRo laboratory and his research interests included bio-signal processing, robotic, wearable robots, neuro-rehabilitation and neural control of movements. He is currently working as a Machine Learning DSP Software Engineer at the Camlin Italy SRL.

Domenico Buongiorno is a Post-Doc Researcher in Electronic and Information Bioengineering at the Department of Electrical and Information Engineering of Polytechnic University of Bari. He received the B.Sc. and M.Sc. (cum laude) degrees in automation and control theory engineering from Politecnico di Bari, Bari, Italy, in 2011 and 2014, respectively. His bachelor and master theses, both supervised by the Prof. Vitoantonio Bevilacqua, concerned machine learning-based optimization techniques for energy consumption optimization and human neuromusculoskeletal modeling, respectively.
In 2017, he received the Ph.D. degree in Emerging Digital Technologies from Scuola Superiore Sant?Anna, Pisa, Italy (PERCeptual RObotics laboratory – PERCRO). His PhD thesis concerns the control of robotic interfaces for interaction with virtual environments, robot-aided neurorehabilitation (EMG based control – Myocontrol) and bilateral multi-DoF teleoperation in disaster scenario. In 2017, he has been a visiting PhD Student at the Biorobotics Laboratory, UCI Irvine, California, under the supervision of the Prof. David Reinkensmeyer. He is currently working on the research projects SOS and RoboVir, and on two industrial projects in collaboration with COMAU Robot Company.
His research interests include human-machine and human-robot interaction, assistive technologies, muscle synergy analysis and myocontrol for neuro-rehabilitation. He teaches Computer Science at the Polytechnic University of Bari (a.y. 2017/2018 and 2018/2019) and Electronic and Information Bioengineering at the Medical School of the University of Bari (a.y. 2018/2019).
In March 2019, he founded Apulian Bioengineering srl, a spin-off company of the Polytechnic University of Bari.

Antonio Frisoli (Eng., PhD) is Full Professor of Robotics and Engineering Mechanics at Scuola Superiore Sant? Anna, where he leads the Human-Robot Interaction area and he is responsible of the Sant'Anna Macronode for the Artes National Competence Center on Collaborative Robotics. He received his PhD (2002) with honors in Industrial and Information Engineering from Scuola Superiore Sant?Anna, Italy and the MSc (1998) in Mechanical Engineering, minor Robotics, from University of Pisa-Italy. His interests in advanced kinematics started with the study of screw theory and Lie algebra applied to the synthesis and study of dynamics of novel parallel kinematics. His research interests are in the field of wearable robotics and haptic interfaces, advanced robotic solutions for inspection, maintenance and disaster scenarios, rehabilitation robotics and advanced kinematics.

Vitoantonio Bevilacqua is Associate Professor of Electronic and Information Bioengineering at the Department of Electrical and Information Engineering of Polytechnic University of Bari (DEI-POLIBA) where obtained the Laurea Degree in Electronic Engineering, Ph.D. in Electrical Engineering and Post-Doc in Industrial Informatics and is the Head of Industrial Informatics Lab. In 2019 he got the National Scientific Habilitation (ASN) as Full Professor of Information Processing Systems.
Since 1996 he has been working and investigating in the field of computer vision and image processing, bioengineering, human-machine interaction based on machine learning and soft computing techniques (neural networks, evolutionary algorithms, hybrid expert systems, deep learning). The main applications of his research are in medicine, in biometry, in bioinformatics in ambient assisted living and industry.